*American Mineralogist, Volume 61, pages 287–294, 1976*

# A molecular orbital study of shared-edge distortions in linked polyhedra

J. A. TOSSELL

*Department of Chemistry, University of Maryland*
*College Park, Maryland 20742*

AND G. V. GIBBS

*Department of Geological Sciences, Virginia Polytechnic Institute and State University*
*Blacksburg, Virginia 24061*

**Abstract**

Molecular orbital results, obtained using an approximate self-consistent-field method, are presented for two systems, one consisting of two silicate tetrahedra sharing a common edge and saturated with hydrogens at their periphery ($Si_2O_6H_4$), and the other, consisting of a silicate tetrahedron sharing an edge with a Mg-containing octahedron and saturated with hydrogens ($SiMgO_8H_{10}$). For both systems the $O_{br}$–Si–$O_{br}$ angle opposite the shared edge has been varied while all distances and angles not involved in the shared edge have been held fixed. For $Si_2O_6H_4$, an energy minimum is found at an $O_{br}$–Si–$O_{br}$ angle of about 85°; this is significantly less than the undistorted value of 109.5° but in fairly good agreement with the observed $O_{br}$–Si–$O_{br}$ angle (93°) in silica-W and $Si_2O_2$. The energy stabilization at this minimum is about 100 kcal/$Si_2O_6H_4$ unit. For $SiMgO_8H_{10}$, the minimum energy obtains when $\langle O_{br}\text{–Si–}O_{br}\rangle \sim 103°$, in good agreement with the observed data for forsterite. For the Si–Mg cluster, the energy stabilization at the minimum is only 4 kcal/$SiMgO_8H_{10}$ unit. An important determinant of total energy is found to be the covalent overlap repulsion between the metal atoms, manifested in large negative bond overlap populations. Decreases in $M$–O bond overlap populations and charge redistribution from $M$ to the exterior of the bridging oxygen atoms also contribute significantly to total energy changes.

## Introduction

Pauling (1929) stated that "The presence of shared edges and particularly of shared faces, in a coordinated structure decreases its stability; this effect is large for cations with large valence and small coordination number, and is especially large in case the radius ratio approaches the lower limit of stability of the polyhedron." This principle, generally known as Pauling's Third Rule, was rationalized from the ionic model and has since been used to explain a large number of crystal chemical observations. The rule has since been amended by Baur (1972) who stated "Ionic structures with shared polyhedral edges and faces can only be stable if their geometry allows the shortening of the shared polyhedral edges. When adjustment stresses force a shared edge to be long, this is a particularly destabilizing feature of the crystal structure." Baur has interpreted the relative stability of the olivine and spinel polymorphs of $(Mg,Fe)_2SiO_4$ in light of this principle. A similar analysis was earlier given by Kamb (1968). Although the olivine polymorph of $(Mg,Fe)_2SiO_4$ contains more shared edges than does the spinel polymorph, the olivine form is more stable because its structure allows for natural reduction of the shared O–O edges and an increase in $M$–$M$ distance, due to the presence of vacant tetrahedral sites. In spinel, such accommodation of bond lengths and angles is apparently not possible. Baur's approach generally emphasizes the importance of distortion stresses produced by the accommodation of polyhedral dimensions, somewhat reducing the importance of specific $M$–$M$ repulsions. Fleet (1974) has attempted to correlate the relative degree of shared edge distortion resulting from various $M$–$M'$ pair repulsions across shared edges with $Q_{eff}/R(M\text{–}M')$, where $Q_{eff}$ is the effective charge of the metal ion. Covalency was thus considered in reducing metal charges from their formal values but other possible covalent effects on equilibrium O–O edge distances and $M$–O–$M'$ angles were ignored. However, the angular distortions presented by Fleet show only a weak dependence on $Q_{eff}/R(M\text{–}M')$ and several anomalies are observed. More recently, Fleet (1975) has found an improved correlation between $\langle O_{br}$–Si–$O_{br}\rangle$ and $Q/R(M$–Si), where $Q$ is the formal charge on ion $M^{Q+}$. Fleet suggested several possible explanations for this correlation. Since the formal charge on an ion equals the number of valence electrons in the neutral atom or the number of bonding electron pairs in the $M$–O cluster (for closed shell compounds), we suggest alternatively that the $M$–$M$ repulsion may be a result of covalent repulsions between the bonding electron pairs in the $M$–O polyhedra. Such repulsion arises from the operation of the Pauli exclusion principle and might reasonably be directly proportional to the number of bonding electron pairs and inversely proportional to the $M$–$M$ distance. The equality between formal charge and number of atomic valence electrons, discussed earlier by Pauling (1960), clearly makes any explanation of this experimental correlation rather ambiguous. In addition it is well-known that a perfect correlation between two experimental variables, in and of itself, cannot establish a cause and effect relationship between them. To establish qualitative cause and effect relationships we feel that quantum mechanical calculations are very useful. We agree however that observed correlations will often be superior for predictive purposes since the quantum mechanical methods and models presently applicable to large systems are quite approximate. We have found that covalent forces are an important factor in the success of the Third Rule and will demonstrate such here using simple approximate SCF (self-consistent field) MO calculations. Such methods have been previously employed by deJong and Brown (1974) in a study of the relative stabilities of corner-, edge-, and face-shared $AlO_6$ double octahedral clusters.

### Molecular orbital methods

The calculations were performed using the SCF-NEMO method, previously described (Tossell, 1973) and the CNDO/2 method (Pople and Beveridge, 1970). The CNDO/2 calculations employed program 141 from the Quantum Chemistry Program Exchange, modified to exclude $d$ orbitals on third row atoms. The SCF-NEMO method has recently been modified to include a uniform sphere of positive charge which surrounds the anion cluster and stabilizes it, so as to give negative values for the energies of all occupied orbitals (Watson, 1958). A scheme has also been added to do a "mixed" MO-ionic calculation by separating the cluster into a "covalent" part which is treated by the MO scheme and an "ionic" part, consisting merely of point charges at fixed positions. The Coulombic potential exerted by the point charge array is calculated at the position of each atom in the "covalent" part of the cluster. This potential is then added to the diagonal elements of the Fock and nuclear-attraction matrices for all the orbitals on the given atom. After self-consistency has been achieved, the Coulombic repulsion between the nuclei of the "covalent" segment and the point charge array is added to the total energy. The perturbation of a central "covalent" cluster by a point charge array can then be studied for those systems which are too large for a complete MO calculation. This approach also allows the separation of point charge effects and covalency effects, but must be used with caution. Changes have also been made in the $K_{ij}$ parameters used to generate the off-diagonal Hamiltonian matrix elements. New $K_{ij}$ values have been obtained from the Fock, kinetic, and overlap matrices generated in the *ab initio* SCF calculation of Collins, Cruickshank, and Breeze (1972), utilizing only an $s,p$ only basis set on Si, *i.e.*, Si $d$ orbitals are excluded in agreement with the conclusions of Tossell (1975).

### Systems studied

The major systems studied were $Si_2O_6H_4$, two edge-sharing silicate tetrahedra with saturating peripheral hydrogens, and $SiMgO_8H_{10}$, a silicate tetrahedron edge linked to a Mg-containing octahedron, with saturating hydrogens (one on each nonbridging O bound to Si and two on each nonbridging O bound to Mg). Several other ancillary calculations, *e.g.* on $Si_2O_6^{4-}$, $SiMgO_8^{10-}$ and $Mg_2O_{10}^{16-}$ were also completed. For the two major calculation sets, wave functions and total energies were obtained for a number of $O_{br}$–Si–$O_{br}$ angles holding $R$(Si–O), $R$(Mg–O), and $R$(O–H) constant at 1.61, 2.12, and 0.96 Å, respectively. For $SiMgO_8H_{10}$ the mean angle $\langle O_{br}$–Mg–$O_{br}\rangle$ was therefore entirely determined by the mean angle $\langle O_{br}$–Si–$O_{br}\rangle$. All $O_{nbr}$–Si–$O_{nbr}$ angles were maintained at 109.5°. Each calculation is time-consuming because of the large number of orbitals involved and the need for iteration to self-consistency. Therefore only a small number of $O_{br}$–Si–$O_{br}$ angles are considered, and the angles corresponding to minimum energies are estimated using a parabolic fit. Curves of total energy *vs.* $\langle O_{br}$–Si–$O_{br}\rangle$ are given in Figures 1a and 4 for $Si_2O_6H_4$ and $SiMgO_8H_{10}$, respectively.

### SCF-NEMO computational results: $Si_2O_6H_4$

Edge-sharing silicate tetrahedra have never been observed in minerals. This fact may be understood qualitatively in terms of the Third Rule; edge-sharing

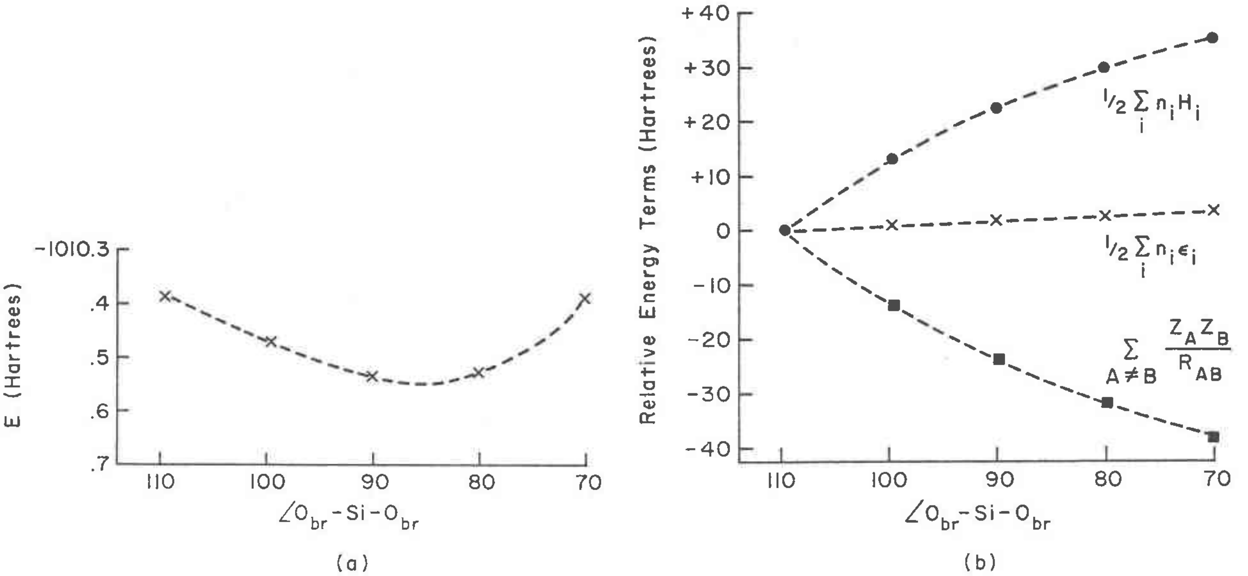


FIG. 1. Variation in (a) total energy and (b) one electron energy, eigenvalue sum and nuclear repulsion energy as a function of the mean angle $\langle O_{br}–Si–O_{br}\rangle$ for $Si_2O_6H_4$ ($H_i = T_i + V_i$).

tetrahedra result in very short *M–M* distances. Therefore the minimum energy for this unstable cluster should occur for an $\langle O_{br}–Si–O_{br}\rangle$ much reduced from the 109.5° tetrahedral angle and the energetic effects should be large and easy to study. In agreement with the qualitative theory, the minimum energy angle calculated using the SCF-NEMO method is indeed very small, about 85°, (with $R$(Si–Si) = 2.37 Å and $R(O_{br}–O_{br})$ = 2.18 Å) as shown in Figure 1, in which energies are given in Hartree units (1 Hartree = 627 kcal/mole). This minimum energy conformation is in fairly good agreement with the $O_{br}–Si–O_{br}$ angle (~93, $\hat{\sigma}$ = 1.5°) observed (1) for the low density fibrous polymorph silica-W which contains molecules of edge-sharing silicate tetrahedra running parallel to the fiber axis (Weiss and Weiss, 1954), and (2) for the high temperature molecule $Si_2O_2$ which contains two Si atoms situated across a shared edge in a rhomboidal complex (Anderson, Ogden, and Kicks, 1968).

The total energy of a system is a complicated quantity given by the equation:

$$E = 1/2 \sum_i n_i\epsilon_i + 1/2 \sum_i n_i(T_i + V_i) + \sum_{A\neq B} \frac{Z_A Z_B}{R_{AB}}$$

where the $n_i$ are MO occupation numbers, $\epsilon_i$, $T_i$, and $V_i$ are the eigenvalue, kinetic energy, and electron-nuclear attraction energy for the $i^{th}$ MO and $Z_A$ is the nuclear charge of atom A. In Figure 1b trends in these separate energy terms are also shown. Clearly none of the separate terms has the same angular dependence as does the total energy. In fact, it is not logically correct to ascribe an observed variation in total energy to any single quantity. However, we could operationally predict trends in the total energy if we could find a quantity giving the same minimum energy angle and about the same magnitude of energy *vs.* angle dependence. Within the ionic model, variations in total energy are determined by variations in the Coulombic energy $\sum_{A\neq B} \frac{Q_A Q_B}{R_{AB}}$ and by variations in Born repulsion between the closed-shell ions. In the MO scheme variations in total energy can be separated into terms corresponding to: (1) a charge redistribution energy, resulting from redistribution of electrons between atomic orbitals with different electronegativities; (2) a Coulombic energy, arising from point-charge effects; and (3) an overlap energy, proportional to overlap populations or interatomic bond orders, and generally separable into bonding, nonbonding, and antibonding components. Gordon (1969) has carried out such an analysis rigorously for the CNDO method. A similar analysis is also qualitatively valid for the SCF NEMO method although less straightforward because of the different approximations used.

The Coulombic energies as a function of bridging angle have been calculated for $Si_2O_6H_4$, using both Mulliken atomic charges from the SCF-NEMO calculations and formal ionic charges, and are shown in Figure 2. To obtain the ionic model total energy we must add to this quantity the Born repulsion be-

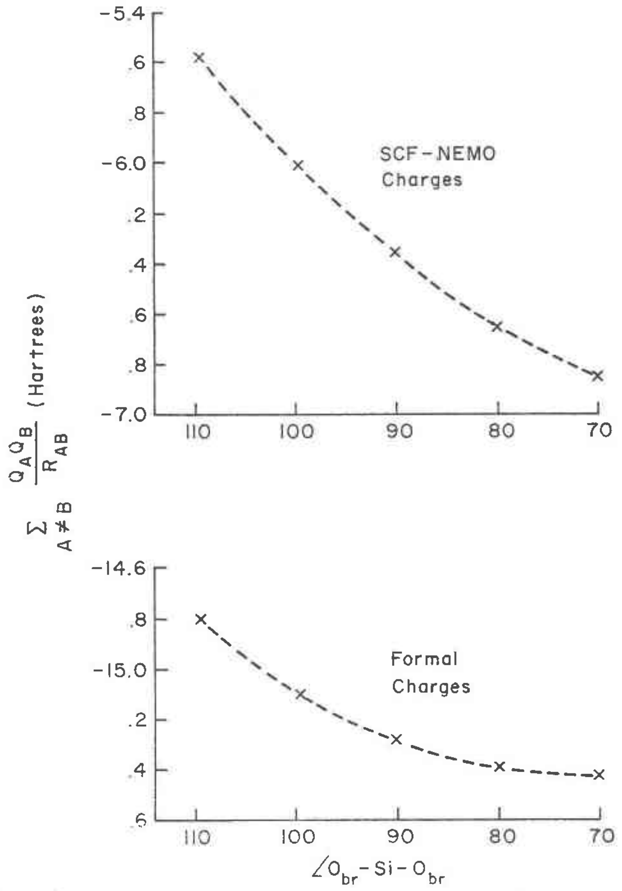


FIG. 2. Variation of point-charge Coulombic energy $\left(\sum_{A \neq B} \frac{Q_A Q_B}{R_{AB}}\right)$ in $Si_2O_6H_4$ as a function of $\langle O_{br}$-Si-$O_{br}\rangle$.

tween the bridging oxygens. Repulsion constants between ions of like charge are difficult to evaluate from experimental data. The most systematic calculations including such repulsion terms were performed by Huggins and Sakamoto (1975). The repulsion energy between like charge ions is, in their terminology, equal to

$$bc_{--} \frac{M'}{2} \exp [a(2r_B - k_2r_O)]$$

where $b = 10^{-12}$ erg/molecule and $c_{--} = 0.5$. For the bridging oxygens in $Si_2O_6H_4$, $M' = 2$ and $k_2r_O$ is the $O_{br}$–$O_{br}$ distance and $a$ and $r_O{}^{2-}$ are repulsion parameters and "constant energy" radii to be determined from experiment. Huggins and Sakamoto give alternative sets of $a$ and $r_O{}^{2-}$ values, giving similar degrees of agreement with experiment. We choose their parameter set $a$ = 3.0 Å and $r_O^{2-}$ = 1.35 Å which gives a maximum $O_{br}$–$O_{br}$ repulsion energy. With this parameter choice, the $O_{br}$–$O_{br}$ repulsions are 0.014, .024, .040, .076, .147, and .303 Hartree units at $O_{br}$–Si–$O_{br}$ angles of 109.5°, 99.5°, 90°, 80°, 70°, and 60°, respectively (the alternative parameter choice gives repulsion energies smaller by a factor of 2-3). This results in a minimum at 78° if the Coulombic energy is evaluated using formal charges but no minimum within the 70–109.5° range if SCF-NEMO charges are used. However much evidence, both spectral (Tossell, 1975) and X-ray (Cooper *et al.*, 1973), suggests that silicates are not completely ionic and that formal ionic charges are never achieved. Therefore the ionic model results using formal charges are of dubious significance.

A simple MO-model term related to the Born repulsion between the bridging oxygens is the overlap population, $n(O_{br}$–$O_{br})$, which rapidly increases in magnitude at small angle. The energy contribution of this term can be estimated by multiplying the overlap population by the average Hamiltonian matrix element of the overlapping orbitals. For a $\langle O_{br}$–Si–$O_{br}\rangle$ of 70°, this term is only about 0.01 Hartrees, much less than the calculated Born repulsion. This suggests that the parameter set chosen exaggerates the Born repulsion. The Si–Si repulsion calculated from $n$(Si–Si) and the Hamiltonian matrix elements is 0.46 Hartrees at 109.5° and is reduced to about 0.05 Hartrees at 70°; this term thus further stabilizes the cluster at small angle. The additional destabilization needed at small angle to balance the changes in SCF-NEMO point charge energy and Si–Si overlap repulsion energy arises both from the transfer of charge from Si to $O_{br}$ and from the reduction in $n$(Si–O). A reduction in angle forces electron density away from Si and the $O_{br}$–$O_{br}$ overlap region and into nonbonding $O_{br}$ orbitals, thus both reducing overlap populations between Si and bridging and nonbridging oxygens and also transferring charge from the more stable Si3$s$ orbital to the less stable O2$p$. These effects are clearly shown by the charge distribution data given in Table 1.

The results for the neutral cluster $Si_2O_6H_4$ may be compared to those for the anion $Si_2O_6^{4-}$, with a stabilizing Watson sphere of charge 4.0 and radius 1.86 Å (chosen to give an eigenvalue of −7 ev for the highest energy occupied orbital). The curve of total energy *vs.* ⟨O–Si–O⟩ (Fig. 3) is quite similar to that for $Si_2O_6H_4$ but the minimum occurs at a slightly greater angle. Examination of the relative energy trends shows a continuous destabilization of the anion with respect to the neutral cluster at small angle. This effect arises from the increased electron repulsion attendant upon contraction of the anion, but no simple way of correcting for it has been found. At-

TABLE 1. Energy and Charge Distribution as a Function of $\langle O_{br}$–Si–$O_{br}\rangle$ in $Si_2O_6H_4$

| $\langle O_{br}$-Si-$O_{br}$ | E | R(Si-Si) | R($O_{br}$-$O_{br}$) | Q(Si) | Q($O_{br}$) | n(Si-$O_{br}$) | n(Si-$O_{nbr}$) | n(Si-Si) | n($O_{br}$-$O_{br}$) |
|---|---|---|---|---|---|---|---|---|---|
| 109.5 | -1010.386 | 1.86 | 2.63 | 2.74 | -1.39 | .175 | .128 | -.850 | -.007 |
| 99.5 | -1010.469 | 2.08 | 2.46 | 2.82 | -1.43 | .156 | .120 | -.365 | -.013 |
| 90.0 | -1010.537 | 2.28 | 2.28 | 2.89 | -1.47 | .143 | .112 | -.200 | -.022 |
| 80.0 | -1010.529 | 2.47 | 2.07 | 2.95 | -1.51 | .133 | .099 | -.130 | -.037 |
| 70.0 | -1010.537 | 2.64 | 1.85 | 2.99 | -1.54 | .126 | .079 | -.090 | -.071 |

tempts at contracting the Watson sphere so as to maintain constant the energies of either the highest occupied MO or the Si or $O_{nbr}$ core orbitals failed to improve the variation of total energy.

In the $Si_2O_6^{4-}$ case, this extraneous electron-repulsion effect is small, since the total charge is small. However for the highly charged cluster $Mg_2O_{10}^{16-}$ the extraneous electron-repulsion effect leads to a continuous decrease in energy as the bridging angle is decreased. In this case the electron-repulsion energy is apparently lowered by reducing $\langle O_{br}$–Mg–$O_{br}\rangle$, thus increasing the separation of the many nonbridging oxygens. Therefore, unless some correction procedure can be found, angular variations for highly charged anions must give erroneous total energies. Note that the total energies will be the only quantities greatly different between the anion and neutral cluster calculations. For $Si_2O_6H_4$ and $Si_2O_6^{4-}$ trends in Mulliken charges and overlap populations were in the same direction, although slightly larger for the anion. Therefore anion calculations will probably give good trends as a function of angle for everything but the most important quantity, the total energy. This is certainly unfortunate since the H-saturated clusters contain more atoms and orbitals, thus requiring more computer time and larger programs. $Mg_2O_{10}H_{16}$ is outside our present computing capabilities but calculations for edge-sharing between a silicate tetrahedron and a magnesium octahedron as the neutral cluster, $SiMgO_8H_{10}$, are just barely possible and will be described below.

To isolate Coulombic and covalency effects existing between the tetrahedral units in the $Si_2O_6^{4-}$ system, we have also performed a "mixed" $Si_2O_6^{4-}$ calculation with a $SiO_4^{4-}$ unit treated by the MO scheme and the other three atoms represented by their SCF-NEMO point charges alone. This calculation should show approximately the same point-charge effects as the full $Si_2O_6^{4-}$ MO calculation but will show no covalent antibonding effects between the two Si atoms or between $O_{br}$ and the second Si. The total energy *vs.* angle curve of Figure 3 shows that in this case the optimum $\langle O_{br}$–Si–$O_{br}\rangle$ is much larger, around 105°. This suggests that a major part of the angular distortion in $Si_2O_6^{4-}$ arises from covalent antibonding forces between the Si atoms. This interpretation is supported by the similarity of trends in calculated charges and bond overlap populations for the full $Si_2O_6^{4-}$ MO calculation and the "mixed" calculation just described. For both calculations we find that $Q$(Si) becomes more positive, $Q(O_{br})$ more negative, $n(O_{br}$–$O_{br})$ more negative and $n$(Si–O) less positive at similar rates as we reduce

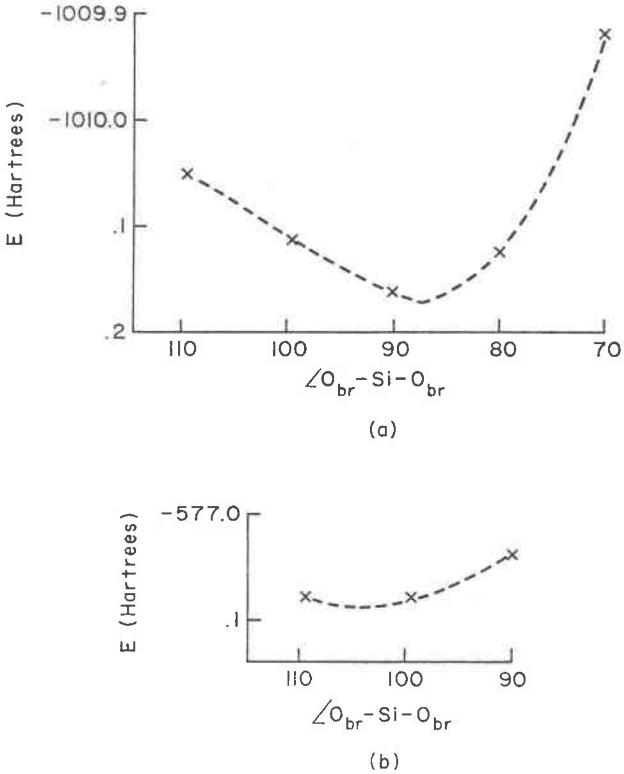


FIG. 3. Variation of total energy in (a) covalent $Si_2O_6^{4-}$ and (b) "mixed" $Si_2O_6^{4-}$($SiO_4^{4-}$ perturbed by point charges at the positions occupied by the other Si and O atoms in $Si_2O_6^{4-}$).

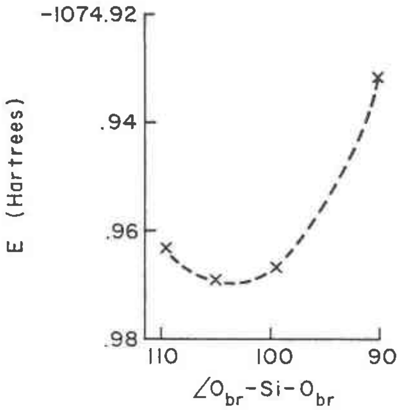


FIG. 4. Variation of total energy *vs.* $O_{br}$–Si–$O_{br}$ angle for $SiMgO_8H_{10}$.

⟨$O_{br}$–Si–$O_{br}$⟩. Therefore the only significant difference between the two calculations is the absence of Si–Si covalent antibonding in the "mixed" case.

## $SiMgO_8H_{10}$

For a silicate tetrahedron sharing an edge with a magnesium octahedron in a hydrogen-saturated $SiMgO_8H_{10}$ cluster, the minimum-energy $O_{br}$–Si–$O_{br}$ and $O_{br}$–Mg–$O_{br}$ angles are 103 and 73°, respectively, with $R(O_{br}–O_{br})$ = 2.52 Å, $R$(Mg–Si) = 2.71 Å, and there is a reduction of energy of 4.4 kcal/$SiMgO_8H_{10}$ from the undistorted value as shown in Figure 4. The geometry of the resulting shared edge conformation is in unexpectedly good agreement with that observed for forsterite (see Table 3) where a silicate tetrahedron shares three of its edges with Mg-containing octahedra. This agreement is pleasantly surprising since the bridging oxygens in the $SiMgO_8H_{10}$ unit would be coordinated by two additional divalent cations in the olivine structure. This suggests that effects internal to the edge-sharing polyhedra dominate the bridging angle. On the other hand, the weak dependence of energy on ⟨$O_{br}$–Si–$O_{br}$⟩ in $SiMgO_8H_{10}$ indicates that external factors could substantially disturb the bridging angle and that the observed agreement of calculation and experiment must be considered cautiously. Using the O–Si–O bending force constants obtained by a normal coordinate analysis of the vibrational spectrum of forsterite (Devarajan and Funck, 1975), we estimate the difference in energy between O–Si–O angles of 109.5° and 103° to be about 1.8 kcal/mole, in reasonable agreement with the calculated value. The point-charge plus Born-repulsion energy shows no minimum for $SiMgO_8H_{10}$ in the angular range 109.5°–90° if SCF-NEMO charges are used. Using formal charges, however, a minimum energy angle of 103° is obtained. This significance of this result is not presently clear to us.

Because the SCF-NEMO method does not lend itself to predicting reliable equilibrium bond lengths, all Si–O bond lengths were held fixed at 1.61 Å and all Mg–O bonds at 2.12 Å. No calculations were made to learn whether the Si–O bonds involved in the shared edges should be longer than those involved in the unshared edges. However, as these bonds are necessarily involved in smaller $\langle O–Si–O \rangle_3$ angles, we anticipate that minimum energy will obtain when the bonds involved in the shared edges are longer than those involved in the unshared ones (Louisnathan and Gibbs, 1971).

The calculated changes in bonding character in $SiMgO_8H_{10}$ are qualitatively the same as in $Si_2O_6H_4$, *i.e.* $M$–O bond overlap populations are reduced and charge is transferred from the $M$ to $O_{br}$ atoms as the bridging angle is closed. The effects are, however, much smaller than in $Si_2O_6H_4$, as is evident from the data in Table 2. For both clusters the $M$–$M$ overlap populations are negative, large, and rapidly increasing at small distance, as shown in Figure 5. They are clearly associated with antibonding interactions, in contrast to the negative O–O overlap populations which are at least ten times smaller and in the range expected for nonbonded atoms. Trends of overlap populations in Si–Si (in $Si_2O_6H_4$) and Si–Mg (in $SiMgO_8H_{10}$) are of similar form and would probably be qualitatively superimposable except for a displacement of the Si–Mg overlap population curve to

TABLE 2. Energy and Charge Distribution as a Function of ⟨$O_{br}$–Si–$O_{br}$⟩ in $SiMgO_8H_{10}$

| <$O_{br}$-Si-$O_{br}$ | E | R(Si-Mg) | Q(Si) | Q(Mg) | Q($O_{br}$) | n(Si-Mg) | n($O_{br}$-$O_{br}$) |
|---|---|---|---|---|---|---|---|
| 109.5 | -1074.963 | 2.59 | 2.85 | .97 | -1.36 | -.259 | -.009 |
| 105.0 | -1074.969 | 2.67 | 2.85 | .97 | -1.36 | -.225 | -.011 |
| 99.5 | -1074.967 | 2.77 | 2.85 | .98 | -1.37 | -.196 | -.015 |
| 90.0 | -1074.932 | 2.93 | 2.87 | 1.00 | -1.37 | -.161 | -.024 |

TABLE 3. The Minimum Energy Angles and Interatomic Separations for the Shared Edge Conformation in $SiMgO_8H_{10}$ Compared with Those Observed for Forsterite

| Minimum Energy Values in $SiMgO_8H_{10}$ Assuming R(Si-O) = 1.61 and R(Mg-O) = 2.12 Å | Values Observed for Forsterite |
|---|---|
| $<O_{br}$-Si-$O_{br}$ = 103° | 102.0(2x),104.8° |
| $<O_{br}$-Mg-$O_{br}$ = 73° | 74.7(2x),71.4° |
| R($O_{br}$-$O_{br}$) = 2.52 Å | 2.56(2x),2.59 Å |
| R(Mg-Si) = 2.71 Å | 2.70(2x),2.80 Å |

longer *M–M* distance by about 0.5 Å, just the difference of the Mg–O and Si–O equilibrium distances. The metal-metal distances in the undistorted $Si_2O_6H_4$ and $SiMgO_8H_{10}$ geometries differ by a larger amount, about 0.73 Å, since edge-sharing leads to shorter relative distances for two tetrahedra than for a tetrahedron and an octahedron (Pauling, 1929). Therefore the overlap repulsion effect and the changes in bonding associated with it must be smaller for edge sharing between a tetrahedron and octahedron.

## CNDO/2 computational results

CNDO/2 calculations give minimum energy $\langle O_{br}$–Si–$O_{br}\rangle$ angles of 78° and 103° for $Si_2O_6H_4$ and $SiMgO_8H_{10}$, respectively. These results will not be discussed in detail since they were performed primarily to check the SCF-NEMO calculations and to establish that our results were not hopelessly method-dependent (although they may well be model-dependent). As in the case of the SCF-NEMO calculations, the *M* atoms become more positive and the $O_{br}$ more negative as the $O_{br}$–Si–$O_{br}$ angle decreases. These trends hold even though the CNDO/2 charges (Si ~1.4, Mg ~.8, O ~−.3 to −.7, H ~.2) are much smaller than the SCF-NEMO. A decrease in angle also decreases the electron density in the Si3*p* orbitals and the $O_{br}2p$ orbital lobes parallel to the Si–*M* axis while increasing the electron density in the $O_{br}2p$ orbital lobes directed away from the molecular center along the $O_{br}$–$O_{br}$ axis. Therefore changes in charge distribution are also similar to those found using SCF-NEMO.

## Conclusion

Curves relating total energy to bridging angle, when calculated by approximate MO methods for the linked polyhedral clusters $Si_2O_6H_4$ and $SiMgO_8H_{10}$, are in good agreement with experiment. *M–M* covalent antibonding effects appear to strongly influence the total energy variation although charge redistribution from Si to $O_{br}$ and reduction of Si–O bond overlap populations are also important.

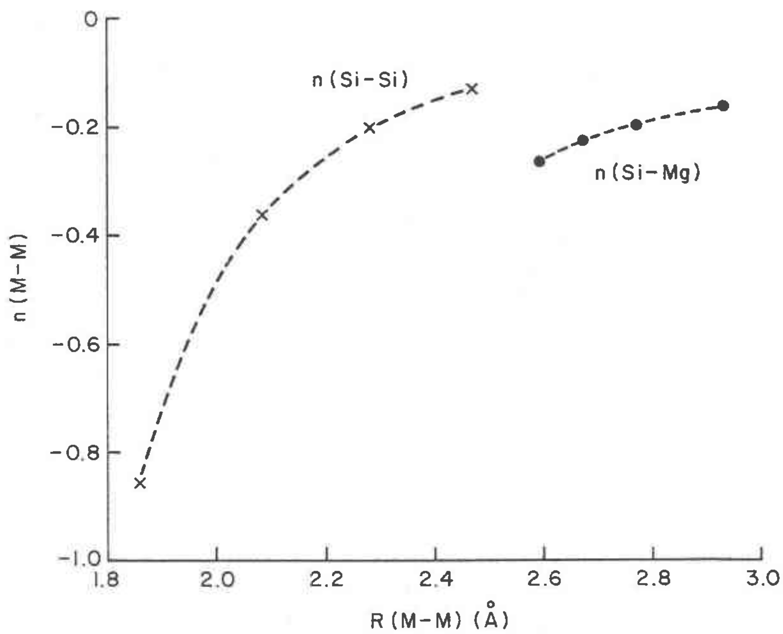


FIG. 5. Overlap population, $n(M–M)$, *vs.* $R(M–M)$ in $Si_2O_6H_4$ (crosses) and $SiMgO_8H_{10}$ (filled circles).

*Note added*

Recent studies using the ionic model (G. J. Dienes, D. O. Welch, C. R. Fischer, R. D. Hatcher, O. Lazareth and M. Samberg, 1975, Shell-model calculation of some point-defect properties in $\alpha$-$Al_2O_3$, *Phys. Rev. B*, **11**, 3060–3070) suggest that the $O^{2-}$–$O^{2-}$ repulsions we have calculated using the Huggins and Sakamoto parameters are much too large. For example, the results of Dienes *et al.* give a $O_{br}^{2-}$–$O_{br}^{2-}$ repulsion of about 0.015 Hartree units for $Si_2O_6H_4$ with $\langle O_{br}$–Si–$O_{br}\rangle = 70°$, compared to our estimate of 0.147. Using the Dienes repulsion values, the sum of the Coulombic energy (from formal charges) plus the $O_{br}^{2-}$ –$O_{br}^{2-}$ repulsion energy shows no minimum within the angular range 109.5 to 70° for $Si_2O_6H_4$ and a minimum at about 97° for $SiMgO_8H_{10}$. The better agreement with experiment obtained using the Huggins and Sakamoto parameters is therefore probably fortuitous.

## Acknowledgments

The computer time for this project was supported partly through the Computer Science Center of the University of Maryland. The authors gratefully acknowledge support from NSF grants GH-33577 and DE571-00486-A03. Helpful discussions were held with G. E. Brown, Jr. Professor D. W. J. Cruickshank is thanked for contributing the computer output from his *ab initio* SFC calculation for $H_4SiO_4$ and for helpful comments on the manuscript. Several useful suggestions were made by the referees, particularly regarding the Born repulsion energy calculation.

## References

ANDERSON, J. S., J. S. OGDEN, AND M. J. KICKS (1968) Infrared spectra and structures of matrix-isolated disilicon, digermanium, and ditin oxides ($Si_2O_2$,$Ge_2O_2$, and $Sn_2O_2$). *Chem. Comm.* **24,** 1585–1586.

BAUR, W. H. (1972) Computer-simulated crystal structures of observed and hypothetical $Mg_2SiO_4$ polymorphs of low and high density. *Am. Mineral.* **57,** 709–731.

BIRLE, J. D., G. V. GIBBS, P. B. MOORE, AND J. V. SMITH (1968) Crystal structures of natural olivines. *Am. Mineral.* **53,** 807–824.

COLLINS, G. A. D., D. W. J. CRUICKSHANK, AND A. BREEZE (1972) *J. Chem. Soc., Faraday Trans.* II, **68,** 1189–1195.

COOPER, W. F., F. K. LARSEN, P. COPPENS, AND R. F. GIESE (1973) Electron population analysis of accurate diffraction data. V. Structure and one-center charge refinement of the light-atom mineral kernite, $Na_2B_4O_6(OH)_2 \cdot 3H_2O$. *Am. Mineral.* **58,** 21–31.

DEJONG, B. H. W. S., AND G. E. BROWN (1974) On Pauling's Third Rule, *Am. Geophys. Union Fall Annu. Meet., EOS,* **56,** 1201.

DEVARAJAN, V., AND E. FUNCK (1975) Normal coordinate analysis of the optically active vibrations (K = O) of crystalline $Mg_2SiO_4$ (forsterite). *J. Chem. Phys.* **62,** 3406–3411.

FLEET, M. E. (1974) Distortions in the coordination polyhedra of *M* site atoms in olivines, clinopyroxenes, and amphiboles. *Am. Mineral.* **59,** 1083–1093.

——— (1975) Bond angle distortions in silicate tetrahedra. *Acta Crystallogr.* **B 31,** 1095–1097.

GORDON, M. S. (1969) A molecular orbital study of internal rotation. *J. Am. Chem. Soc.* **91,** 3122–3130.

HUGGINS, M. L., AND Y. SAKAMOTO (1957) Lattice energies and other properties of crystals of alkaline earth chalcogenides. *J. Phys. Soc. Japan,* **12,** 241–251.

KAMB, B. (1968) Structural basis of the olivine-spinel stability relation. *Am. Mineral.* **53,** 1439–1455.

LOUISNATHAN, J. S., AND G. V. GIBBS (1971) Variations in Si–O distances in olivines, sodamelilite, and sodium metasilicate as predicted by semi-empirical molecular orbital calculations. *Am. Mineral.* **57,** 1643–1663.

PAULING, L. (1929) The principles determining the structure of complex ionic crystals. *J. Am. Chem. Soc.* **51,** 1010–1026.

——— (1960) *The Nature of the Chemical Bond,* 3rd ed. Cornell University Press, Ithaca, N.Y., p. 547–548.

POPLE, J. A., AND D. L. BEVERIDGE (1970) *Approximate Molecular Orbital Theory,* McGraw-Hill, N.Y.

TOSSELL, J. A. (1973) Interpretation of *K* X-ray emission spectra and chemical bonding in oxides of Mg, Al, and Si using quantitative molecular orbital theory. *Geochim. Cosmochim. Acta,* **37,** 583–594.

——— (1975) The electronic structures of Si, Al and Mg in tetrahedral coordination with oxygen from SCF-X$\alpha$ MO calculations, *J. Amer. Chem. Soc.,* in press.

WATSON, R. E. (1958) Analytic Hartree-Fock solutions for $O^=$ *Phys. Rev.* **111,** 1108–1110.

WEISS, A., AND A. WEISS (1954) Über eine neue Siliziumdioxyd-Modifikation mit Faserstruktur und Kettenmolekeln. *Naturwissenschaften,* **41,** 12.

*Manuscript received, May 29, 1975; accepted for publication, October 8, 1975.*